JET ANALYSIS*

By P. Hoyer

Nordita, Copenhagen**

(Received September 25, 1979)

The various theoretical descriptions of jets are discussed, including lowest order and leading logarithm calculations in QCD, as well as phenomenological models for non-perturbative fragmentation. Recent results concerning jet broadening, general branching equations and alternatives to the quark cascade model are emphasized.

1. Introduction

It is now about four years since experimental evidence for jet structure was first presented in e^+e^- annihilations [1, 2]. The hadron momenta were found to be aligned with a "jet axis", distributed like $1+\cos^2\theta$ to the beam direction. This strongly suggested a quark fragmentation picture, in which hadrons taking a fixed fraction of the quark energy are produced with limited transverse momenta to the quark direction. Since then, quark jets have been seen in other "hard" scattering processes, namely in deep inelastic lepton-nucleon scattering and in large p_T hadron scattering[1].

Data from the new e^+e^- machines PETRA and PEP will make it possible to study 15 ... 20 GeV jets. First results [4] already indicate that jets become more "pencil-like" at high energies, thus simplifying phenomenological analyses of their properties. These prospects, together with the profound theoretical insights that can be obtained, mean that jet physics will be an active field in the near future.

The theoretical approaches to quark (and gluon) fragmentation can be characterized by the kinematic region in which they are expected to apply:

A. Short time scales: Perturbative QCD.
   1. Lowest order calculations.
   2. Leading logarithm resummations.

B. Long time scales: Nonperturbative hadronization.

---

* Presented at the XIX Cracow School of Theoretical Physics, Zakopane, June 3–17, 1979.

** Address: Nordita, Blegdamsvej 17, DK-2100 Copenhagen Ø, Denmark.

[1] Reviews on the experimental and theoretical status of jets can be found in Ref. [3].

The physics at short time scales (large momentum transfers) offers exciting possibilities for testing Quantum Chromodynamics [5] (QCD). Certain features of the predictions at the parton level are expected [6] to be insensitive to details of the hadronization mechanism. They can thus be tested directly using hadron distributions.

The hadronization models are more phenomenological, and build on experience gained from the study of low-p_T hadron collisions (which also involve long time scales). It is of considerable interest to find whether there are some universal features that are common to both these types of processes.

This is not intended to be a complete review of the subject. I shall discuss both QCD and hadronization models, but the emphasis will in each case be on recent applications. To make the lectures self-contained I shall, however, present the necessary background and ideas. In Section 2 the general features of the data are recalled, together with their interpretation in the parton model [7]. A qualitative discussion of QCD effects is then given in Section 3.

Section 4 describes QCD jet broadening to $O(\alpha_s)$. We find [8] that the increase in $\langle p_T \rangle$, the average transverse momentum, should begin around $E_{CM} \approx 15$ GeV in e^+e^- annihilations, and be a sizeable (100%) effect by $E_{CM} = 30$ GeV.

A convenient way of formulating leading log calculations in terms of branching equations is given [9] in Section 5. I derive a master equation for the generating functional of parton distributions, and discuss its applications.

In Section 6, I discuss a model [10] for hadronization which is closely related to the multiperipheral models of hadron collisions. This model can be solved analytically in the region of the rapidity plateau. The solution has some non-trivial and interesting features, such as a "phase transition" point at which long range correlations arise.

A summary and conclusions are given in Section 7.

2. *Data and the parton model*

Jet phenomena can be studied in all processes where energetic partons are produced. The most common ones are e^+e^- annihilations, deep inelastic scattering of e, μ or ν on nucleons, and hadron-hadron scattering involving high-p_T particles in the final state.

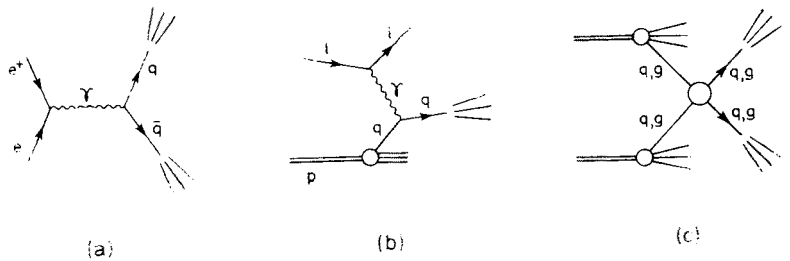

Fig. 1. Hard scattering processes. (a) $e^+e^- \to$ hadrons. (b) Deep inelastic lepton scattering: $lp \to l+X$. (c) Large p_T hadron scattering

The e^+e^- reaction (Fig. 1a) is simple to analyze, as the produced state is pure $q\bar{q}$. It does, however, have the draw-back (from our point of view) that all species of quark q (which are above threshold) have comparable production cross-sections. It is usually quite difficult to determine the quark species on an event-by-event basis [11]. Hence the experimental fragmentation functions are averaged over the quark type, and the situation is further complicated by weak decays of heavy quarks [12].

In deep inelastic scattering (Fig. 1b) the main scattering is off valence quarks in the nucleon. Hence the quark species is well-defined. For charged current ν interactions even the charge of the quark is known. A disadvantage compared to e^+e^- annihilations is the presence of spectator particles from the nucleon wave function. The jet energies are also lower than those soon to be achieved in PETRA and PEP ($E_q^{max} \simeq 19$ GeV).

The situation in large-p_T hadron collisions (Fig. 1c) is complicated by the fact that the hard scattering can involve gluons as well as quarks. If sufficient understanding can be achieved, this will be a unique way of measuring quark-gluon and gluon-gluon scattering. New calorimeter experiments at Fermilab and at the CERN ISR, as well as the huge energies to be achieved in the $p\bar{p}$ colliders should make jet studies particularly fruitful.

Because of confinement, the produced quarks and gluons fragment into a jet of observable hadrons. In the parton model [7], the time-scale for this hadronization is assumed

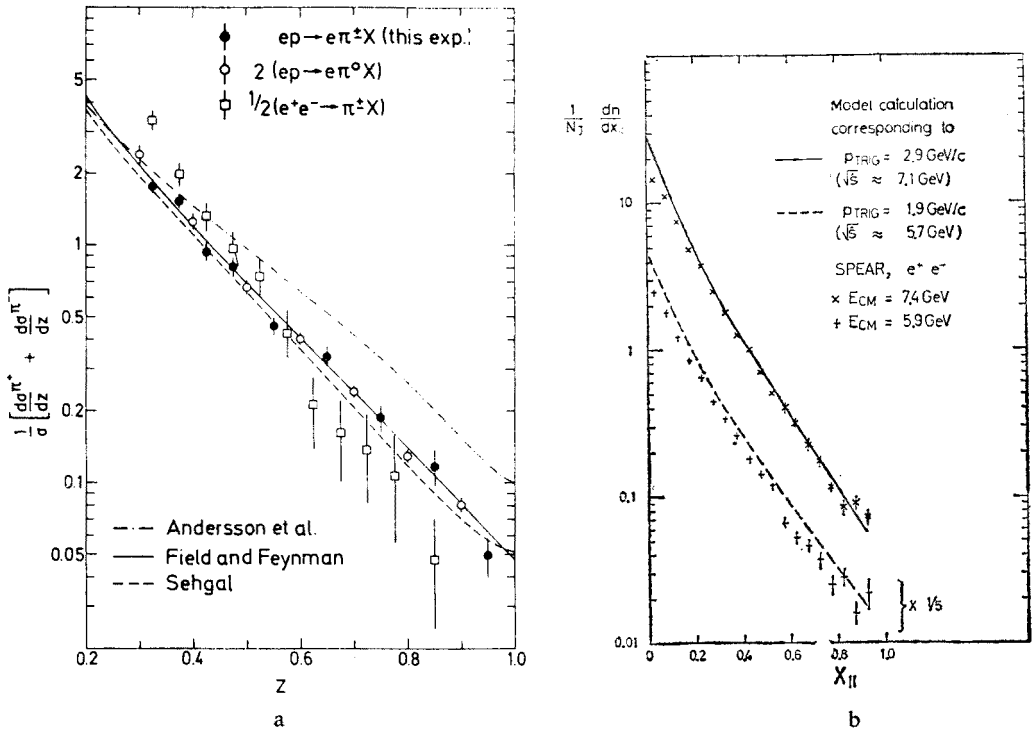

Fig. 2. Comparison of fragmentation functions in different hard processes. (a) $ep \to e+\pi+X$ and $e^+e^- \to \pi+X$ (from Ref. [13]) (b) Model parametrization [14] of charged particle distributions in large p_T pp events (solid and dashed lines) compared to e^+e^- data

to be much longer than that of hard scattering. Hence the two processes are effectively factorized. It follows that hadronization should have several simple features:
(*i*) *Universality*: Jet fragmentation is independent of how the parton was produced.
(*ii*) *Limited* p_T: The natural scale is given by the Fermi motion of quarks inside hadrons $\sim$350 MeV.
(*iii*) *Scaling*: The hadron energy distribution should depend only on the fraction $x = E_h/E_q$ of the quark energy.

The data that has been obtained so far is indeed in qualitative agreement with (*i*) ... (*iii*). Evidence [13, 14] for the universality of fragmentation functions in e^+e^-, deep inelastic and hadron scattering is shown in Fig. 2. As I mentioned above, however, the experimental definition of the "fragmentation function" is not identical in the three processes. This, together with finite energy effects (choice of scaling variable), etc., means that one should regard Fig. 2 only as a rough comparison.

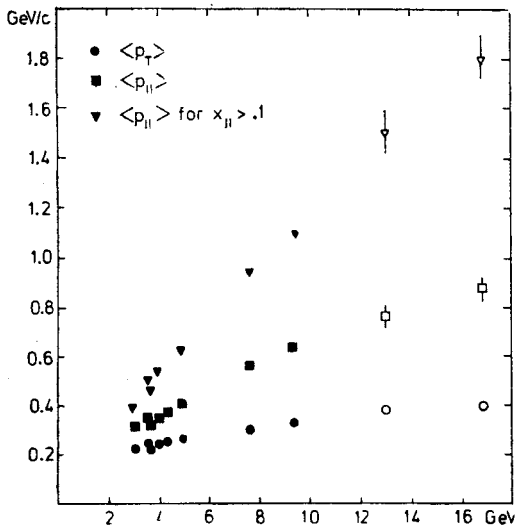

Fig. 3. Average longitudinal and transverse momentum in e^+e^- collisions as a function of c.m. energy [4]

There is at present [4] no clear indication of a rise in $\langle p_T \rangle$ with increasing energy[2] (Fig. 3). The slight increase in $\langle p_T \rangle$ for e^+e^- annihilations at 13 and 17 GeV could be due to bottom decays, for example.

Scaling appears to work well for $x \geqslant 0.2$ in e^+e^- annihilations [4] (Fig. 4). The experimental accuracy is not high, however, and could well hide moderate scale-breaking. Some violation of scaling has been seen [16] in deep inelastic ν scattering (but at low values of W).

[2] Data reported [15] after this school from PETRA on e^+e^- annihilations at 27.5 GeV apparently do show such a rise, however.

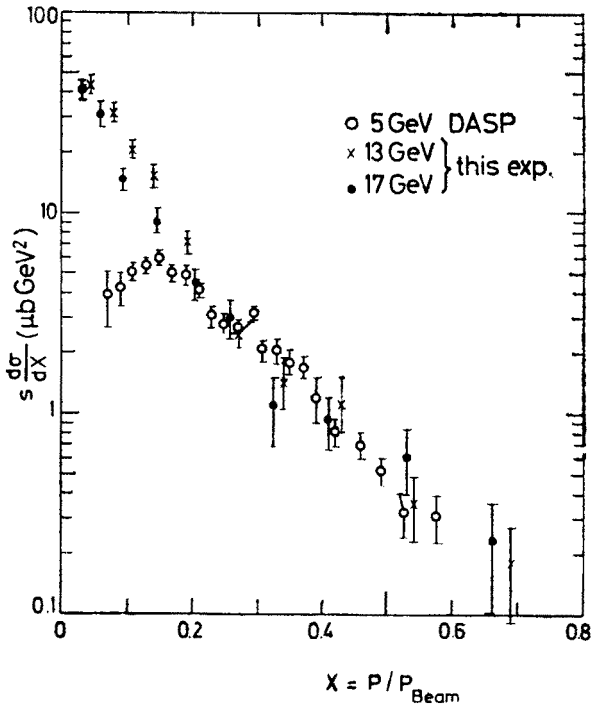

Fig. 4. Comparison [4] of x-distributions of charged particles at Q = 5,13 and 17 GeV

Jet phenomenology today is thus in a situation analogous to that for deep inelastic scattering before violations of Bjorken scaling were discovered. As we shall next discuss, scale-breaking is required by asymptotically free field theories such as QCD. It should become manifest in the data as accuracy and/or energy increases.

3. *QCD effects*[3]

In the parton model one assumes that a nearly on-shell $q\bar{q}$ pair is produced at the photon vertex in $e^+e^- \to$ hadrons[4]. Since the quarks have high energies they live for a long time before turning into hadrons. This is not usually the case in a field theory. One or both of the quarks may be highly virtual and decay in a *short* time interval. Thus in QCD there is to $O(\alpha_s)$ a state containing three nearly on-shell partons (Fig. 5), namely a $q\bar{q}$ pair plus a gluon (g). If all momenta point in distinct directions we would expect the event to give rise to three jets.

A 3-jet event has no preferred axis: p_T and p_L are of the same order. Since such events

[3] Some good reviews are listed in Ref. [17].

[4] For definiteness, I shall in the following limit the discussion to e^+e^- annihilations. Similar arguments apply to the other processes.

contribute a fixed fraction of the total cross-section, apart from the logarithmic decrease of α_s, it is clear that asymptotically,

$$\langle p_T \rangle \sim Q/\log Q, \tag{3.1}$$

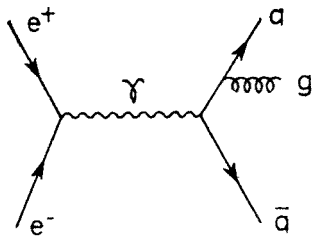

Fig. 5. An $O(\alpha_s)$ diagram for the gluon bremsstrahlung process $e^+e^- \to q\bar{q}g$

where $Q \equiv E_{CM}$. This is a dramatic (power-law!) violation of the parton model assumption $\langle p_T \rangle \sim$ const., and should be observable even with moderate statistics. In Section 4 we discuss this and other $O(\alpha_s)$ effects in more detail, and try in particular to estimate the energy range at which (3.1) should start to apply.

Because of the smallness of α_s, 3-jet events are not very frequent. However, it can be easily seen[5] that $\sigma(q\bar{q}g)$ is sizeable in the region where the gluon momentum is nearly parallel to one of the quark momenta. Neglecting for a moment the quark mass m_q, the virtual quark propagator in Fig. 5 has the denominator

$$(p_q + p_g)^2 = 2p_q \cdot p_g = 2E_q E_g(1 - \cos\theta) \sim \theta^2 \quad \text{for} \quad \theta \to 0.$$

Hence the propagator diverges as $1/\theta^2$ when θ, the angle between the quark and gluon momenta, goes to zero. On the other hand, for transverse gluons the $q \to q + g$ vertex vanishes like θ in the forward direction: the massless quarks conserve their helicity, forcing all collinear gluons to be longitudinal. In a transverse gauge we can thus estimate the contribution to $\sigma(q\bar{q}g)$ from the diagram of Fig. 5 squared,

$$\sigma(q\bar{q}g) \sim \alpha_s \int_{\theta_{min}} \theta d\theta \left(\frac{\theta}{\theta^2}\right)^2 \sim \alpha_s \log \theta_{min} \sim \alpha_s \log (Q/m_q). \tag{3.2}$$

The extra logarithm in (3.2) compensates the decrease in α_s. Consequently $\sigma(q\bar{q}g)$ remains a finite fraction of $\sigma(q\bar{q})$ even at asymptotic energies, and there is no reason to believe in the usual perturbation expansion. There are two ways out of this dilemma:
(*i*) Consider sufficiently inclusive quantities, such as total cross-sections, "jet" cross-sections [6, 19] or the like. For these, it turns out that the logarithms cancel between the contributing final states. Low order calculations in α_s are then meaningful. This is case (A1) mentioned in the Introduction, and we return to it in Section 4.
(*ii*) We may sum all contributions of order $(\alpha_s \log Q)^n$, neglecting terms of higher powers

[5] The following argument is taken from Ref. [18].

of α_s without compensating log's. This is the leading logarithm approximation[6] (l.l.a.). It is feasible to do this because the leading logarithms come from a very restricted region of phase space, where all momenta are nearly collinear. Furthermore, interference terms can be neglected in axial gauges. In our example this is clear since such terms have one less power of θ/θ^2 in (3.2).

Because of the absence of interference terms the l.l.a. has a very simple probabilistic interpretation. The diagrams to be squared and summed are of the type shown in Fig. 6a (together with vertex and propagator corrections, which transform the coupling constant

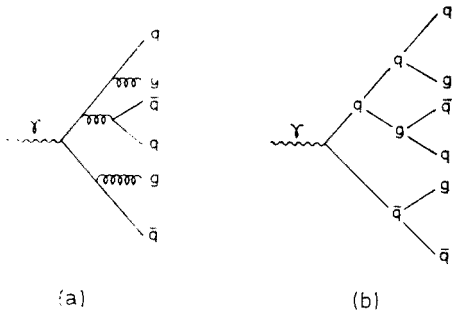

Fig. 6. (a) Diagram contributing to multi-parton production. (b) The corresponding branching process

α_s into the running one $\alpha_s(Q^2)$). The corresponding physical process is shown in Fig. 6b: The photon first fragments into $q+\bar{q}$, subsequently the quarks independently emit gluons, and so on. The fact (which of course must be established by explicit calculation) that all fragments of a given generation decay independently makes this into a *branching process* [21] (Fig. 6b). This is the starting point for our discussion in Section 5.

The leading logarithms come from the region where all momenta are nearly parallel: We are looking at the structure of a single (fixed-angle) jet. The number of generations, or "branching time", is measured by the virtual mass of the partons. As seen in (3.2), large logarithms imply that the ratio of fragment to parent masses in each decay must be a small number, say of order $\delta(\ll 1)$:

$$\log \theta_{\min} \sim \log (m_{\text{final}}/m_{\text{initial}}) \sim \log \delta.$$

After t decays, the typical parton mass is

$$m_t \sim \delta^t Q. \tag{3.3}$$

The magnitude of the virtual mass m determines the transverse spread of the decay products through the kinematic relation

$$m^2 = \sum_i \frac{m_i^2 + \vec{p}_{iT}^2}{x_i}. \tag{3.4}$$

[6] For reviews see Ref. [20].

Here the sum is over all decay products of mass m_i, transverse momentum p_{iT} and energy fraction x_i ($\sum_i x_i = 1$). In this way the transverse momentum of a final particle labels the "time" t at which its parent parton was produced. This has been used to study the transverse spread of jets [22], and also provides a simple way [23] of summing the leading logarithms in the Sterman–Weinberg problem [6].

It follows from (3.3) and (3.4) that the spread of decay products from partons of late generations t will be small. We may think [24] of these partons as forming smaller jets within the overall fixed-angle jet. It is still an open question whether, at sufficiently high energy, such substructure within jets could actually be detected experimentally.

The partons will presumably continue to branch until their masses reach some fixed value of order 1 GeV, at which point non-perturbative phenomena take over. The total branching time is thus, using (3.3),

$$t \sim \log (Q/1 \text{ GeV}). \tag{3.5}$$

As we shall see in Section 5, however, the running coupling constant implies that the effective time increases only as $\log \log Q$.

With each decay, the virtual mass drops by a large factor $1/\delta$, whereas the energy is more or less evenly shared between the final particles. Hence the final, nearly on-shell partons are still quite energetic. It is then reasonable to assume that the hadronization of those partons bears some resemblance to soft hadron collisions.

Most of the work done on the hadronization aspect has so far been based on the quark cascade model [11, 25], which was originally proposed [26] for hadron collisions. New and higher energy data will make such studies even more important. One should compare general features of the two types of processes, and see whether successful scattering models can be applied to parton hadronization. In Section 6 we discuss a few such questions, and investigate a specific, multiperipheral-type model for jets.

4. Jet broadening

I. Infra-red safe cross-sections

As we saw above (Eq. (3.2)), exclusive cross-sections in general have factors $\log (Q/m_q)$ that spoil the convergence of the perturbation expansion in the $Q \to \infty$ limit. Alternatively, we could say that the cross-section is singular as $m_q \to 0$. The origin of such singularities is well-known already from investigations [27] of QED. They can be eliminated by summing over all energy-degenerate final (and initial) states. To $O(\alpha_s)$ with $m_q = 0$, these are states where one quark is replaced by a quark plus a collinear or soft gluon (Fig. 7).

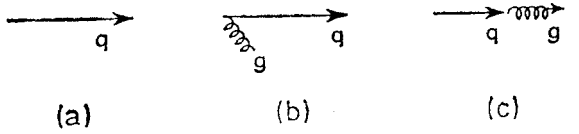

Fig. 7. The three energy-degenerate states occurring in lowest order. (a) Single quark. (b) Quark plus soft gluon. (c) Quark plus hard collinear gluon

The simplest example of an "infra-red safe" cross-section, for which a sum over degenerate states is implied, is that of the total e^+e^- annihilation rate

$$\sigma_{TOT} = \sigma_{Born}\left[1 + \frac{\alpha_s}{\pi} + O(\alpha_s^2)\right].$$

It is indeed free of logarithms, and the reliability of the perturbation expansion is usually taken for granted.

As was pointed out by Sterman and Weinberg [6], much "less inclusive" cross-sections can be defined, which are nonetheless infra-red safe. Their QCD jet cross-section comprised events having all but a fraction ε of the total CM energy within a cone of half-opening angle δ. Since soft gluons can be emitted in any direction, and a quark can be replaced by a quark plus a gluon moving in the same direction, without changing the event classification, the cross-section is infra-red finite. An explicit calculation [6] showed that the jet cross-section indeed was free of infra-red singularities. Terms of $O(\varepsilon)$ and $O(\delta)$, which were neglected in the original calculation, have since been included [28]. A summation of all leading $\log \delta$ terms has also been done [23] (up to $O(\varepsilon)$).

As $Q \to \infty$, $\alpha_s \to 0$ and the perturbation expansion for infra-red safe cross-sections converges rapidly. It is then plausible [6, 19] to assume that the QCD prediction, which is calculated in terms of parton final states, holds also for the physical (hadron) cross-section. Thus we have an excellent possibility of testing QCD experimentally: These predictions should be insensitive to the (so far) poorly understood non-perturbative effects. Several alternative definitions of infra-red safe cross-sections have by now been suggested [17, 29, 30].

In practice, it may be difficult to do the tests at presently accessible energies. From the measured opening angle of the jets [2, 30] and from the fact [4] that $\langle p_T \rangle$ does not increase with Q it appears that non-perturbative effects dominate jet production even in the $Q = 10 \ldots 15$ GeV range. At upper PETRA/PEP energies perturbative effects could become important. It is unlikely, however, that non-perturbative phenomena can be neglected until considerably higher (LEP?) energies.

With today's data in mind it is therefore useful to study how and when the emerging QCD effects manifest themselves above the non-perturbative "background". Such an analysis will clearly be more model dependent than the jet predictions discussed above. In the work [8] that I shall describe here, we tried three different ways of merging the perturbative and non-perturbative effects. Encouragingly, all three methods lead to consistent results concerning p_T broadening and other QCD phenomena. We therefore believe that they are reliable first estimates.

II. $e^+e^- \to q\bar{q}g$

To facilitate the following discussion, let me begin by reminding [19, 31] you of the kinematics and dynamics of the $O(\alpha_s)$ QCD process $e^+e^- \to q\bar{q}g$ (Fig. 5). I shall use massless kinematics throughout.

The q, $\bar{q}$ and g momenta lie in a plane, the production plane. The orientation of this plane w.r.t. the e^+e^- beam axis is specified by QCD. It is different for vector and scalar

gluons and can thus be used to test the gluon spin [8, 17, 32]. Here I shall, however, assume that these angles are averaged over. The event configuration is then completely specified by the scaled energies

$$x_i = \frac{2E_i}{Q} \quad (0 \leqslant x_i \leqslant 1) \quad i = \mathrm{q}, \bar{\mathrm{q}}, \mathrm{g} \tag{4.1}$$

which satisfy

$$x_{\mathrm{q}} + x_{\bar{\mathrm{q}}} + x_{\mathrm{g}} = 2. \tag{4.2}$$

The usual definition of *thrust* T for a final state with many hadrons h is [33]

$$T = \max \frac{\sum_{\mathrm{h}} |p_{\parallel}^{\mathrm{h}}|}{\sum_{\mathrm{h}} |\vec{p}_{\mathrm{h}}|}. \tag{4.3}$$

Here the maximization is done w.r.t. the direction along which the components $p_{\parallel}^{\mathrm{h}}$ are measured. The maximal direction is called the *thrust axis.*

The definition (4.3) can be applied also to a parton final state in QCD. Since T is linear in the momenta, it takes the same value for energy-degenerate states. Just as we discussed above, this implies that the singularities cancel. Thrust is an "infra-red safe variable" whose value is (hopefully) not much changed by the hadronization process. This is to be contrasted with sphericity S,

$$S = \tfrac{3}{2} \min \frac{\sum_{\mathrm{h}} |\vec{p}_{\mathrm{T}}^{\mathrm{h}}|^2}{\sum_{\mathrm{h}} |\vec{p}_{\mathrm{h}}|^2}, \tag{4.4}$$

which was the variable first used by experimenters [1]. For hadron final states, the S and T axes turn out to be nearly the same. However, in QCD sphericity is a singular variable (for massless quarks).

For the $\mathrm{q\bar{q}g}$ final state it is readily seen that

$$T = \max_i (x_i)$$

and the thrust axis is parallel to the momentum of the most energetic parton. The transverse momentum p_{T} of the two other partons w.r.t. the T axis is given by

$$p_{\mathrm{T}}^2 = \frac{Q^2}{T^2} (1 - x_{\mathrm{q}})(1 - x_{\bar{\mathrm{q}}})(1 - x_{\mathrm{g}}). \tag{4.5}$$

A hadron which is a fragment of such a parton has, in addition to (4.5), an intrinsic (non-perturbative) p_{T} w.r.t. the parton. A straightforward calculation shows that the transverse momentum of the hadron w.r.t. the thrust axis is, averaging over the non-perturbative fragmentation,

$$p_{\mathrm{T}}^2 = \langle p_{\mathrm{T}}^2 \rangle_{\mathrm{NP}} + \tfrac{1}{4} [\langle x_{\parallel}^2 \rangle_{\mathrm{NP}} x^2 Q^2 - 2 \langle p_{\mathrm{T}}^2 \rangle_{\mathrm{NP}}] \sin^2 \theta. \tag{4.6}$$

Here $\langle\ \rangle_{NP}$ denotes the average for non-perturbative (NP) fragmentation, and $x_{||}$ is the hadron's scaled longitudinal momentum. x, θ are the parton's scaled energy and angle to the thrust axis.

The QCD cross-section for $e^+e^- \to q\bar{q}g$ to $O(\alpha_s)$ is, integrating over the e^+e^- beam direction [31],

$$\frac{1}{\sigma_{Born}} \frac{d\sigma(q\bar{q}g)}{dx_q dx_{\bar{q}}} = \frac{2}{3} \frac{\alpha_s}{\pi} \frac{x_q^2 + x_{\bar{q}}^2}{(1-x_q)(1-x_{\bar{q}})}. \tag{4.7}$$

The collinear and soft gluon singularities are explicitly seen in the limits $x_q, x_{\bar{q}} \to 1$.

III. The overall $\langle p_T^2 \rangle$

At first thought, one might expect the $\langle p_T^2 \rangle \propto Q^2$ behavior (3.1) to set in at quite low energies, $Q \sim$ a few GeV, sufficient to produce gluons of 1 GeV or so. However, Eq. (4.6) reminds us of an important fact: the coefficient of Q^2 is proportional to $\langle x_{||}^2 \rangle_{NP}$. The gluon must be sufficiently energetic to produce *hadrons* with transverse momenta above the NP ones. Since the hadron energy fraction $\langle x_{||}^2 \rangle_{NP} \sim 0.04$ is small [1], the p_T increase for hadrons sets in at rather high energies[7].

To obtain a quantitative estimate of the rise in $\langle p_T^2 \rangle$ due to QCD we shall make use of the KLN theorem [27]. All singularities will cancel provided the energy-degenerate states in Fig. 7 are given equal weights. In our case this means that we must assume that the three states give rise to the same hadron $\langle p_T^2 \rangle$. If the partons fragment independently, this is plausible for the single quark and the soft gluon states. In the case of collinear gluons, it requires that $\langle p_T^2 \rangle_{NP}$ is the same in quark and gluon hadronization. While these assumptions cannot be expected to be rigorously valid, we do believe that they are reasonable for an estimate of the energy scales.

With the above assumption, it is straightforward to calculate the $\langle p_T^2 \rangle$ of hadrons w.r.t. the thrust axis using (4.6) and (4.7). Taking $\langle p_T^2 \rangle_{NP}$ and $\langle x_{||}^2 \rangle_{NP}$ from e^+e^- data [1] at $Q = 7$ GeV we find

$$\frac{\langle p_T^2 \rangle}{\langle p_T^2 \rangle_{NP}} = 1 + \frac{1}{\log(Q/\Lambda)} \left[\left(\frac{Q}{14.3\ \text{GeV}} \right)^2 - 0.2 \right], \tag{4.8}$$

where $\Lambda \approx 0.5$ GeV. The large energy scale ~ 15 GeV is due both to the small $\langle x_{||}^2 \rangle_{NP}$ and to the scarcity of hard gluons. As seen from Fig. 8, the increase in $\langle p_T^2 \rangle$ is only a moderate effect for $Q \lesssim 17$ GeV, in qualitative agreement with data. Already at 30 GeV $\langle p_T^2 \rangle$ has increased by a factor two, however. This effect should be clearly visible at PETRA and PEP[8,9].

---

[7] This is also a reason for why the two-jet structure of e^+e^- events is seen [1] only for $Q \gtrsim 6$ GeV.

[8] After this school was held, results were reported [15] from PETRA at $Q = 27.4$ GeV. The data indeed shows a $\langle p_T^2 \rangle$ broadening consistent with Fig. 8. It also agrees with the $\langle p_T^2(z) \rangle$ prediction to be discussed below (Fig. 10).

[9] Other phenomena, such as the weak decay of a new heavy quark, also lead [12] to increasing $\langle p_T^2 \rangle$. If top quarks are produced it could prove difficult to determine the QCD effect quantitatively.

An analogous calculation was done for $\langle p_T^4 \rangle$. This result is also shown in Fig. 8. The scale turns out to be essentially the same as for $\langle p_T^2 \rangle$, but the rise is of course much more rapid ($\propto Q^4$). On the other hand, higher statistics is needed to measure $\langle p_T^4 \rangle$ accurately.

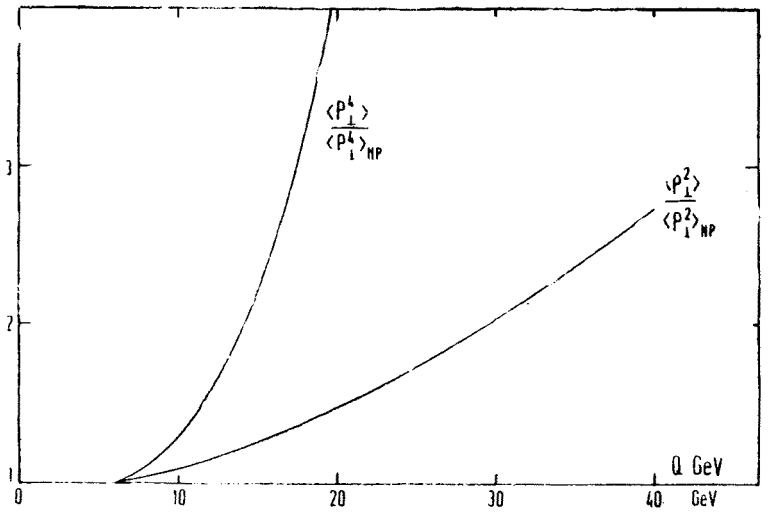

Fig. 8. The energy dependence of $\langle p_T^2 \rangle$ and $\langle p_T^4 \rangle$ obtained [8] from QCD to $O(\alpha_s)$

IV. The seagull effect

It is natural to expect that most of the p_T increase from gluon bremsstrahlung will be reflected in the fast hadrons. We should thus consider $\langle p_T^2(z) \rangle$, the average transverse momentum of hadrons with a fixed energy fraction[10] $z = 2E_h/Q$. One characteristic of gluon bremsstrahlung is immediately obvious from the Feynman diagram of Fig. 5: To $O(\alpha_s)$, p_T increases in only one hemisphere. Hence, given the thrust axis, we should for each event define the "narrow" and the "broad" hemisphere by considering the value of thrust in a given hemisphere H:

$$T_H = \max \{ \sum_{i \in H} |p_\parallel^i| / \sum_{i \in H} |\vec{p}^i| \}. \tag{4.9}$$

As the energy grows, $\langle p_T^2(z) \rangle$ should increase in the "broad hemisphere" and remain constant in the "narrow" one.

For a quantitative estimate, we note that when Q^2 is large we can simplify Eq. (4.6) for p_T^2 to

$$p_T^2 = \tfrac{1}{4} z^2 Q^2 \sin^2 \theta. \tag{4.10}$$

The approximation breaks down for $\theta \lesssim \langle p_T \rangle_{NP}/zQ$, i.e. in the region where the perturbative cross-section (4.7) is itself unreliable. We shall calculate $\langle p_T^2(z) \rangle$ using (4.7) and (4.10)

[10] A similar quantity has been considered in Ref. [34], using another method.

over the whole kinematic domain, and estimate how much the result depends on the region of small p_T [11].

If we write

$$\langle p_T^2(z)\rangle - \langle p_T^2(z)\rangle_{NP} = \frac{\alpha_s(Q^2)}{\pi} G(z) Q^2, \tag{4.11}$$

then

$$G(z) = \tfrac{4}{3} z^2 \int_{2/3}^{T_0} \frac{dT}{T^2} \int_{x_L}^{T} \frac{dx}{x^3} \left\{ [\varrho(T, x) + \varrho(x, 2-T-x)] D_q\left(\frac{z}{x}\right) + \varrho(2-T-x, T) D_g\left(\frac{z}{x}\right) \right\} \Big/ D_q(z), \tag{4.12}$$

where $x = \max\{z, 2(1-T)\}$ and

$$\varrho(x_1, x_2) = \frac{x_1^2 + x_2^2}{(1-x_1)(1-x_2)} (1-x_1)(1-x_2)(x_1+x_2-1).$$

The thrust cut-off T_0 eliminates the region where the gluon is nearly parallel to the quarks. We estimate T_0 to be the point where the thrust distributions of two- and three-jet

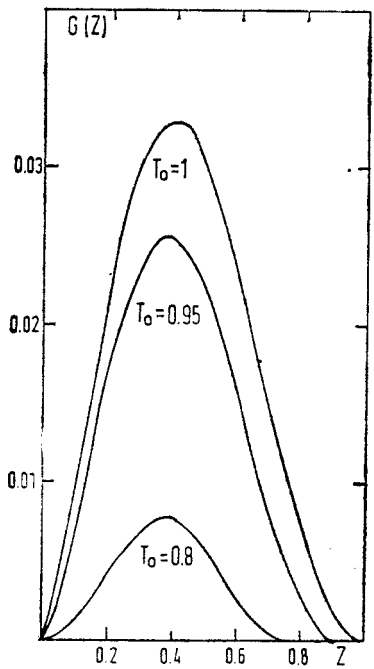

Fig. 9. The dependence of the function $G(z)$ in Eq. (4.12) on the cut-off T_0

[11] Eventually, higher order (in α_s) multi-jet cross-sections limit the region of applicability of (4.7) to the exterior of a cone of fixed *angle*, rather than fixed p_T (cf. the discussion above). However, the present $O(\alpha_s)$ calculation is sufficient for a study of the onset of QCD effects.

events merge when NP fragmentation is included (see below). We find then

$$T_0 = 0.92 \quad (Q = 15 \text{ GeV}), \tag{4.13}$$

$$T_0 = 0.95 \quad (Q = 30 \text{ GeV}).$$

The results for $G(z)$ turn out not to be very sensitive to the form of the fragmentation functions. In the following we use $D_q(z) = D_g(z) = 3(1-z)^2/z$. In Fig. 9 the dependence of $G(z)$ on T_0 is shown. For $T_0 \gtrsim 0.95$, $G(z)$ is only weakly dependent on the cut-off.

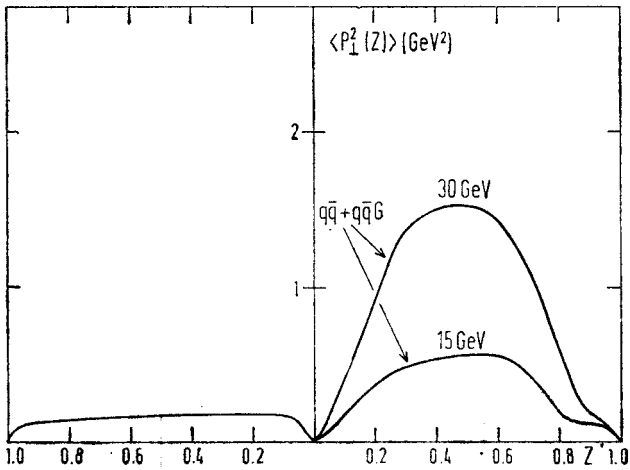

Fig. 10. The average transverse momentum $\langle p_T^2(z)\rangle$ of hadrons with a fixed energy fraction z

We conclude that our results should be reliable for $Q \gtrsim 30$ GeV, and uncertain to perhaps a factor 2 at 15 GeV due to the dependence on T_0.

The prediction for $\langle p_T^2(z)\rangle$ is given in Fig. 10. As in the above consideration of the overall $\langle p_T^2\rangle$, the QCD effect is small at $Q = 15$ GeV. By $Q = 30$ GeV, however, the asymmetry of the distribution is unmistakable. This should, then, be a characteristic prediction of QCD that could not be confused with weak decays.

V. A Monte Carlo model

The third approach to QCD effects that I would like to mention is a Monte-Carlo study. We generate $q\bar{q}$ and $q\bar{q}g$ events according to the QCD cross-sections, and then let the partons hadronize as in the quark cascade model of Field and Feynman [11]. Since entire events are generated, the effect of gluon radiation on any distribution can be obtained. Compared to the above studies, however, a larger number of phenomenological assumptions must be made.

The total $q\bar{q}g$ rate generated was based on (4.7),

$$\sigma(q\bar{q}g) = \int_{2/3}^{T_0} dT \, \frac{d\sigma(q\bar{q}g)}{dT},$$

where T_0 is the NP cut-off. Since we neglect $O(\alpha_s^2)$ effects, the remaining cross-section is $q\bar{q}$ production:

$$\sigma_{q\bar{q}} = \left(1 + \frac{\alpha_s}{\pi}\right)\sigma_{\text{Born}} - \sigma(q\bar{q}g).$$

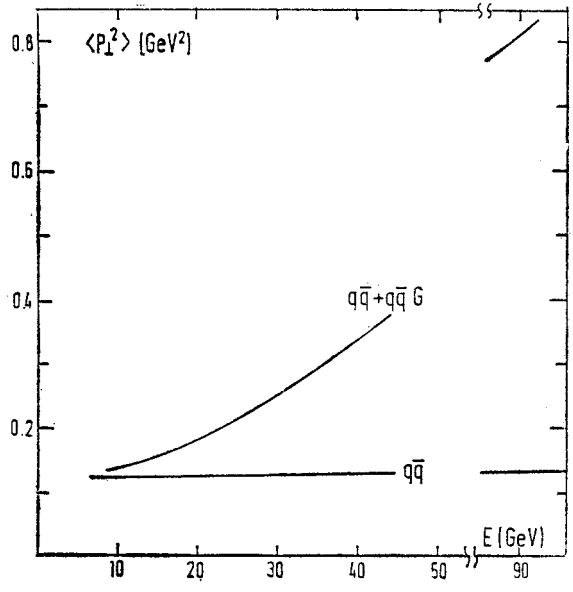

a

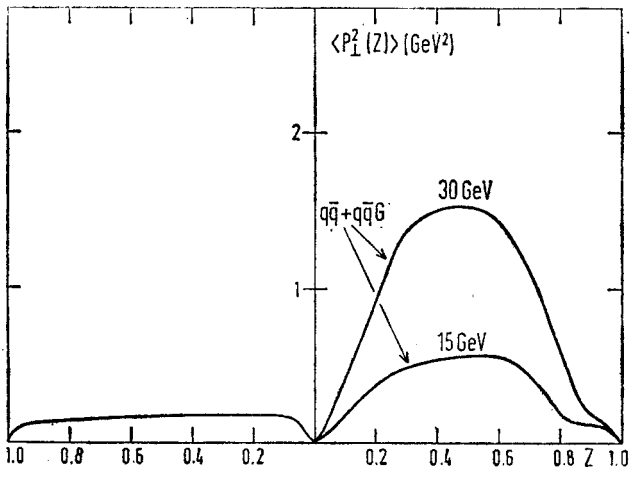

b

Fig. 11. (a) The overall $\langle p_T^2 \rangle$ and (b) $\langle p_T^2(z) \rangle$ as obtained in Monte Carlo jet simulation

The choice of T_0 is to a certain extent arbitrary. We found that a smooth transition from 3-jet to 2-jet events could be obtained with T_0 chosen be to at the maximum of the NP $q\bar{q}$ thrust distribution,

$$\frac{d}{dT}\left[\frac{d\sigma(q\bar{q})_{NP}}{dT}\right]_{T_0} = 0.$$

This gives the T_0 values quoted in (4.13)[12].

The energy dependence of the overall $\langle p_T^2 \rangle$ and of $\langle p_T^2(z) \rangle$ is shown in Fig. 11. They agree very well with the estimates obtained above. The observability of three distinct jets can be judged from the angular energy flow diagrams [19] in Fig. 12. This shows the energy distribution projected onto the $q\bar{q}g$ plane, with the axes determined by the two most energet-

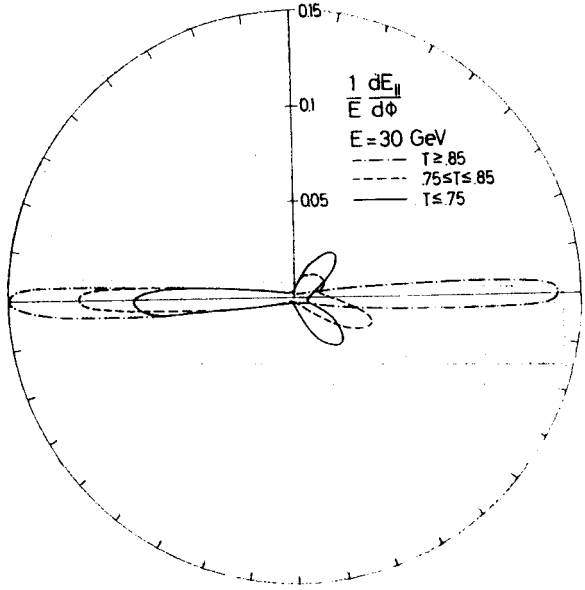

Fig. 12. Angular energy flow as a function of thrust T at $Q = 30$ GeV

ic partons. Three jets are clearly seen at $Q = 30$ GeV. (The significance of such plots must of course be tested by comparing with structures which arise from fluctuations in isotropic (phase-space) distributions.)

In conclusion, we have estimated the onset of gluon radiation effects using three different approaches. Each of them involves assumptions about the NP distributions. Significantly, however, the three methods give very consistent results. Bremsstrahlung begins to emerge above the NP background around $Q = 15$ GeV, and is very important at 30 GeV. The reason for the rather large energy scale is the scarcity of hard gluons and the soft fragmentation spectrum.

[12] The primordial decay function for gluons in the cascade model was taken to be $f(z) = 3(1-z)^2$.

The effects discussed above are significant well inside the PETRA/PEP energy range. If they are not observed experimentally much of the current use of QCD perturbation theory would have to be questioned.

5. Partons and branching

As I indicated in Section 3, QCD calculations can be extended to high orders in α_s in the leading logarithm approximation (l.l.a.). The relevance of this approximation at current energies can certainly be questioned. On the other hand, the qualitative (and quantitative?) success [35] of QCD scaling violations in deep inelastic scattering is encouraging. Furthermore, the conceptual simplification that occurs in the l.l.a. can be a valuable guide.

There are several good reviews of the leading log approach [20]. Here I would like to show how, once the probabilistic nature of the problem has been established, one may reach the answer in a straightforward way [9]. This method[13] can be regarded as a natural generalization of the parton evolution equations derived by Lipatov [37] and Altarelli, Parisi [38], and is in some respects complementary to the "Jet Calculus" of Konishi, Ukawa and Veneziano [39].

In Section 3, I sketched how in the l.l.a. the full contribution comes from squares of diagrams like Fig. 6a, and therefore can be thought of as a branching process [21], Fig. 6b. The salient feature of branching processes is that all fragments that exist at a given "time" evolve independently: the decay probability of tone fragment does not depend on any other fragment. Branching processes have been extensively studied mathematically and found numerous applications.

For conciseness I shall assume a single parton species in the following discussion — the generalization to several species is immediate and will be given below. We consider

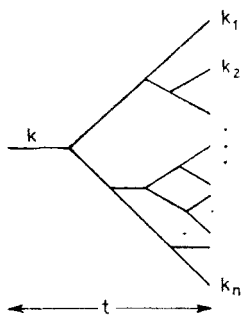

Fig. 13. A parton branching process $k \to k_1 + k_2 + \ldots + k_n$ in time t

the branching process of Fig. 13: What is the probability $P(k \to k_1, \ldots, k_n; t)$ that a parton with initial momentum k fragments into n partons of momenta $k_1, \ldots, k_n$ in time t? The (small) transverse momentum component is averaged over, and "time" is related to the

[13] Similar ideas have recently been proposed in Refs. [36].

virtual mass as in Eqs. (3.3) and (3.5). Since we assume that the initial parton was produced in a hard collision, its mass is $O(|\vec{k}|)$.

It turns out to be simplest not to consider the above probabilities directly, but rather the generating functional defined in terms of them:

$$F(k, \phi, t) = \sum_{n=1}^{\infty} \int dk_1 \ldots dk_n P(k \to k_1, \ldots, k_n; t) \delta(\sum_1 k_i - k) \phi(k_1) \ldots \phi(k_n)/n!. \quad (5.1)$$

Here $\phi(k)$ is a function that can be varied arbitrarily. It is clear that the fragmentation probabilities can be deduced once $F(k, \phi, t)$ is known for all ϕ.

Actually, F has a simple intuitive meaning: It can be regarded as the outcome of an experiment with "acceptance" $\phi(k)$ for observing a parton of momentum k. For example, if the acceptance is unity, all outcomes are measured with probability one and conservation of probability implies

$$F(k, \phi = 1, t) = 1. \quad (5.2)$$

On the other hand, for $\phi(k) = \theta(\lambda - k)$ only partons with momenta less than λ are accepted. F is then the probability that *all* partons at time t have momenta less than λ. This is an example of a probability that has a simple physical meaning, yet is difficult to express in terms of inclusive multi-parton distributions. The inclusive distributions are, however, easy to obtain from F. The single parton distribution is

$$D(k \to xk, t) = \left. \frac{\delta F(k, \phi, t)}{\delta \phi(xk)} \right|_{\phi = 1} \quad (5.3)$$

and multi-parton distributions are obtained by repeated functional differentiation.

At $t = 0$ there is a single parton of momentum k. The initial condition for F is thus

$$F(k, \phi, t = 0) = \phi(k). \quad (5.4)$$

We now want to derive an evolution equation for F. The probability for a parton to decay in time dt is

$$dP(k \to xk, (1-x)k; dt) = dt \frac{\alpha(t)}{2\pi} \frac{P(x)}{k}. \quad (5.5)$$

Here $\alpha(t) \sim \frac{1}{t}$ is the running coupling constant, evaluated at Q^2 = parton (mass)^2. This dependence on t means that the decay probability is not constant during the branching. We can, however, eliminate the variation by choosing a new time scale Y,

$$dY = dt \frac{\alpha(t)}{2\pi}. \quad (5.6)$$

Since $Y \sim \log t$, the total branching time on this scale grows like log log Q^2.

The function $P(x)$ in (5.5) can be calculated from the basic field theory vertices. For QCD this has been done by Altarelli and Parisi [38]. If N is the number of colors,

$$P(\mathrm{q} \to \mathrm{q}(x)+\mathrm{g}(1-x)) = \frac{N^2-1}{2N}\,\frac{1+x^2}{1-x},$$

$$P(\mathrm{g} \to \mathrm{q}\bar{\mathrm{q}}) = \tfrac{1}{2}\,[x^2+(1-x)^2],$$

$$P(\mathrm{g} \to \mathrm{gg}) = 2N\,\frac{(1-x+x^2)^2}{x(1-x)}. \tag{5.7}$$

The characteristic soft gluon singularity is explicit in (5.7). The derivation below of the evolution equation for $F(k, \phi, Y)$ is strictly valid only for vertex functions $P(x)$ without such a singularity. However, the final result can be written in a form which remains meaningful for vertices like (5.7) with infra-red singularities. No further "regularization" is then necessary.

The generating functional at time dY is, using (5.1), (5.5) and neglecting the contribution from states with more than two partons (which is $O(dY^2)$),

$$F(k, \phi, dY) = \left(1-\frac{dY}{T}\right)\phi(k)+\frac{dY}{2}\int_0^1 dx P(x)\phi(xk)\phi((1-x)k). \tag{5.8}$$

The "life-time" T can be obtained by imposing (5.2) on (5.8):

$$\frac{1}{T} = \tfrac{1}{2}\int_0^1 dx P(x). \tag{5.9}$$

Thus, "$T = 0$" for vertices like (5.7) with infra-red singularities.

From (5.8), the time derivative of F at $Y = 0$ is

$$\frac{d}{dY}F(k, \phi, Y)|_{Y=0} = -\frac{1}{T}\phi(k)+\tfrac{1}{2}\int_0^1 dx P(x)\phi(xk)\phi((1-x)k). \tag{5.10}$$

We still have to find the analog of (5.10) at arbitrary Y. This can be immediately done using a convolution property of the generating functional for branching processes, which I shall next describe.

The evolution of a branching process can be divided into two steps (Fig. 14). The probability of a final state $\{k_i\}$ at time Y_1+Y_2 is obtained by summing over all possible intermediate states $\{\hat{k}_i\}$ at time Y_1,

$$P(k \to k_1, \ldots k_n; Y_1+Y_2) = \sum_{\hat{k}_i} P(k \to \hat{k}_1, \ldots, \hat{k}_m; Y_1)P(\hat{k}_1 \to \ldots; Y_2)$$

$$\times P(\hat{k}_2 \to \ldots; Y_2) \ldots P(\hat{k}_m \to \ldots; Y_2). \tag{5.11}$$

A sum over all (inequivalent) ways of assigning the final partons $\{k_i\}$ as decay products of the intermediate partons $\{\hat{k}_i\}$ is implied. The fact that the partons at Y_1 evolve independently has been used in writing the decay probability as a product.

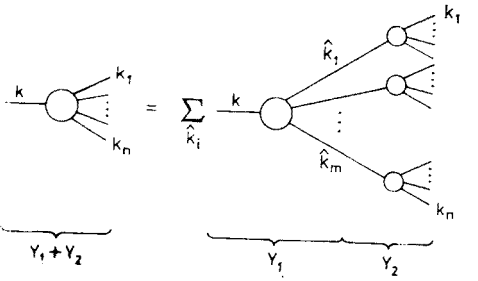

Fig. 14. Completeness relation for branching processes

If we multiply both sides of (5.11) by the product $\phi(k_1) \ldots \phi(k_n)$ and sum over all states $\{k_i\}$, the l.h.s. becomes $F(k, \phi, Y_1+Y_2)$ (cf. (5.1)). On the r.h.s., we get a product $F(\hat{k}_1, \phi, Y_2) \ldots F(\hat{k}_m, \phi, Y_2)$. When this is combined with $P(k \to \hat{k}_1, \ldots \hat{k}_m; Y_1)$ and summed over $\{\hat{k}_i\}$, we get another $F(k, \phi, Y_1)$ in which, however, each $\phi(\hat{k}_i)$ is replaced by $F(\hat{k}_i, \phi, Y_2)$.

In other words: The evolution of k into $\{k_i\}$ in time Y_1+Y_2 can be done by first evolving k into $\{\hat{k}_i\}$ during Y_1. This implies $\phi(k) \to F(k, \phi, Y_1)$. Then each parton at Y_1 evolves a further time Y_2: $\phi(\hat{k}_i) \to F(\hat{k}_i, \phi, Y_2)$. Formally we can express this as

$$F(\phi, Y_1+Y_2) = F(F(\phi, Y_2), Y_1). \tag{5.12}$$

It is now straightforward to boost the evolution equation (5.10) to an arbitrary time Y. We use

$$\frac{d}{dY} F(\phi, Y) = \frac{d}{dY'} F(\phi, Y+Y')|_{Y'=0} = \frac{d}{dY'} F(F(\phi, Y), Y')|_{Y'=0}. \tag{5.13}$$

Substituting (5.10) in (5.13) we have the general evolution equation

$$\frac{d}{dY} F(k, \phi, Y) = -\frac{1}{T} F(k, \phi, Y) + \tfrac{1}{2} \int_0^1 dx P(x) F(xk, \phi, Y) F((1-x)k, \phi, Y). \tag{5.14}$$

Using (5.9) we may eliminate the life-time T in (5.14),

$$\frac{d}{dY} F(\phi, k, Y) = \tfrac{1}{2} \int_0^1 dx P(x) \left[F(xk, \phi, Y) F((1-x)k, \phi, Y) - F(k, \phi, Y)\right]. \tag{5.15}$$

This is our master equation. Together with the initial condition (5.4) it determines $F(k, \phi, Y)$ at all Y.

Eq. (5.15) is well-defined also for vertices $P(x)$ that have $1/x$ and $1/(1-x)$ singularities like in QCD, provided only that energy-degenerate states are summed over. As usual, this means that the acceptance for soft quanta is unity,

$$\lim_{k\to 0} \phi(k) = 1. \tag{5.16}$$

Since the momenta of the fragments are always less than that of the initial parton, it follows from (5.2) and (5.16) that

$$\lim_{k\to 0} F(k, \phi, Y) = 1. \tag{5.17}$$

This is sufficient to ensure the convergence of the integral in (5.15) even for vertices with infra-red singularities.

Discussion

The evolution equation for single parton distributions follows from (5.15) using (5.3). By scale invariance,

$$D(k \to xk, Y) = \frac{1}{k} D(1 \to x, Y) \equiv \frac{1}{k} D(x, Y). \tag{5.18}$$

Differentiating (5.15) w.r.t. $\phi(xk)$ and setting $\phi = 1$ we get

$$\frac{d}{dY} D(x, Y) = \tfrac{1}{2} \int_0^1 dy P(y) \left[\frac{1}{y} D\left(\frac{x}{y}, Y\right) + \frac{1}{1-y} D\left(\frac{x}{1-y}, Y\right) - D(x, Y) \right]. \tag{5.19}$$

This can be recognized as the Lipatov–Altarelli–Parisi equation [37, 38]. It is interesting to note that the regularization came almost for free in our approach: The singularities in $P(y)$ do not need a $(\ )_+$ prescription[14].

The master equation (5.15) can be readily generalized to the case of more than one parton species. The equation is shown symbolically in Fig. 15, with labels to indicate the

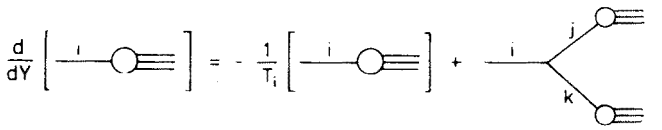

Fig. 15. The master equation (5.20) for the case of several parton species

parton type. There is one acceptance function $\phi_i(k)$ for each species, and several decay functions $P_{i\to jk}(x)$. If $F_i(k, Y)$ is the functional for a branching starting with an initial parton i, we get the set of coupled equations

$$\frac{d}{dY} F_i(k, Y) = \sum_{j,k} \tfrac{1}{2} \int_0^1 dx P_{i\to jk}(x) \left[F_j(xk, Y) F_k((1-x)k, Y) - F_i(k, Y) \right]. \tag{5.20}$$

[14] This has been observed also in Ref. [40].

In contrast to the single parton equation (5.19), the master equations (5.15), (5.20) are non-linear. They can therefore in general not be solved exactly, e.g. by the method of moments [38]. An explicit and non-trivial solution is known [21, 41], however, for the case when $\phi(k) = z$ is independent of k. In this case F reduces to a multiplicity generating function,

$$F(k, z, Y) = \sum_{n=1}^{\infty} z^n P_n(Y), \tag{5.21}$$

where $P_n(Y)$ is the probability to have n partons at time Y. It is easy to verify that

$$F(k, z, Y) = \frac{z}{z+(1-z)\exp(Y/T)} \tag{5.22}$$

is the solution of (5.14). From (5.22) we can find, for example, the average multiplicity

$$\langle n \rangle = \left.\frac{dF}{dz}\right|_{z=1} = \exp(Y/T).$$

The appearance of the life-time T reminds us that the multiplicity is not a finite quantity in theories with infra-red singularities like QCD: We should not count the number of soft gluons.

Although the master equation cannot be solved analytically, it is not difficult to find an approximate numerical solution. If in (5.15) we treat k as a discrete index ($k = 1, \ldots, N$), the equation becomes a set of N first-order coupled differential equations, which can be efficiently solved on a computer. The integrand in (5.15) can be sampled only at the chosen discrete momenta, so that a suitable integration routine is needed (we used Simpson's rule).

This method of solution of course applies equally well to the single parton evolution (5.19), where it is an alternative to moment inversion techniques. Actually, in applications to data the present method has an advantage. The evolution of $D(x, Y)$ depends only on the values of $D(z, Y)$ for $z \geqslant x$, as is clear from (5.19). For calculating moments, on the other hand, the full z-range is required, and this can mean needless extrapolation of data.

We have tested the above method using two vertex functions,

$$P(x) = \frac{1}{x(1-x)} \quad \text{("QCD")}$$

and

$$P(x) = x(1-x) \quad (\phi_6^3). \tag{5.23}$$

The former is qualitatively similar to the $g \to gg$ vertex function in QCD (cf. (5.7)). The latter is appropriate [39] for a ϕ^3 theory in six dimensions (which is also asymptotically free). The evolution of the single parton distribution is shown [15] in Figs. 16. In the "QCD" case one can see how soft gluon emission has removed the initial parton peak by $Y = 1.0$. In ϕ_6^3, on the other hand, the initial peak remains at all times, albeit with exponentially decreasing probability.

[15] To facilitate the numerical integration the initial parton distribution was triangular, peaking at $x = 0.98$ and with a base of 0.04. We used $N = 100$ points.

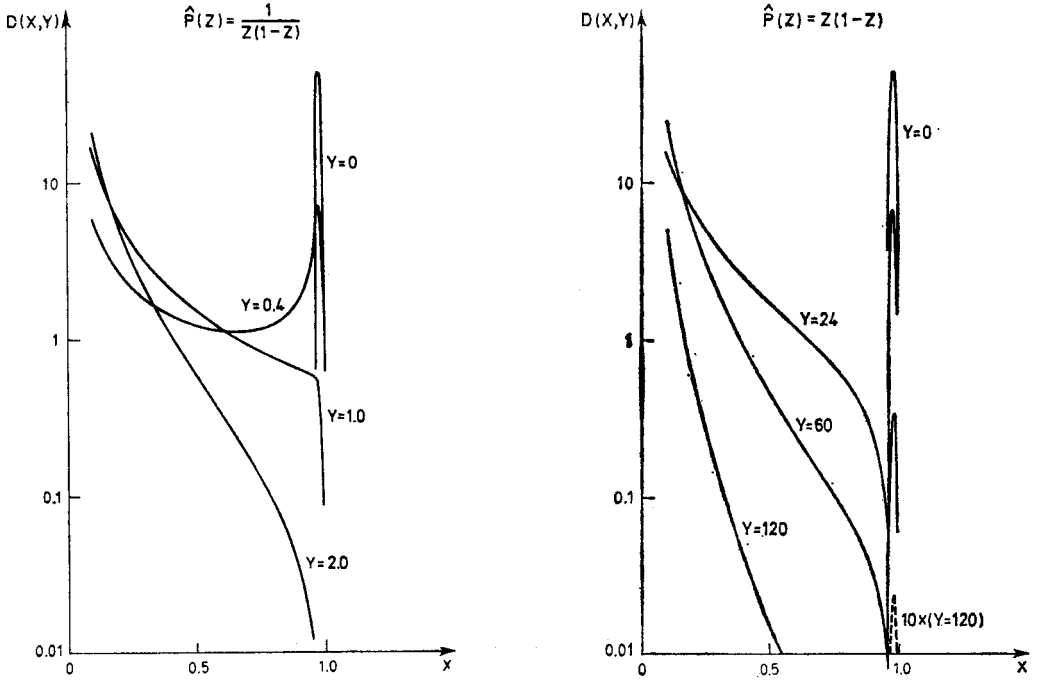

Fig. 16. Single parton inclusive distributions at various times for (a) $P(x) = 1/x(1-x)$. (b) $P(x) = x(1-x)$

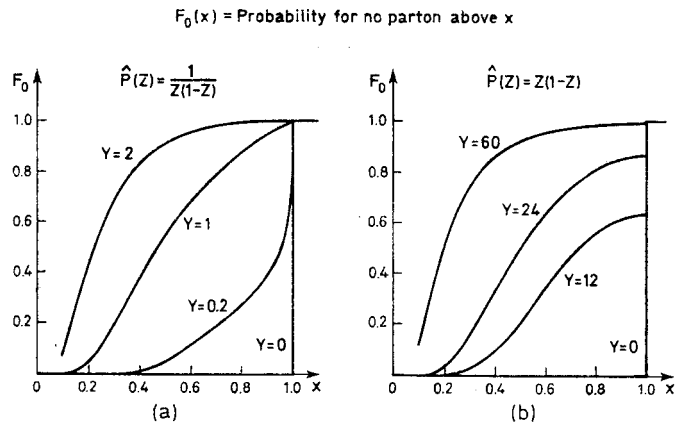

Fig. 17. The probability $F_0(x)$ that there is no parton with fractional momentum greater than x. $F_0(x) = \theta(x-1)$ at $Y = 0$. (a) $P(x) = 1/x(1-x)$. (b) $P(x) = x(1-x)$

The probability $F_0(x)$ that no parton has momentum above x is shown in Fig. 17. This was obtained using $\phi(k) = \theta(x-k)$, as mentioned above. Due to soft gluon emission in "QCD", the likelihood is unity that the initial parton has moved below $x = 1$, for any $Y > 0$. In ϕ_6^3, this probability approaches unity according to the life-time $T = 12$. Away from $x = 1$, however, the two sets of distributions are qualitatively similar.

The above examples illustrate the kind of questions concerning jet evolution that can be answered using the master equation (5.15). It would be interesting to make a phenomenological study with the true QCD vertex functions (5.7). In the present approach one can go beyond single-parton distributions to investigate the over-all structure of the branching. However, for a comparison with experiment some assumption is required concerning how the partons turn into hadrons.

6. *Hadronization*

I. The rapidity plateau

After the hard parton has shaken off its excess mass by rapid bremsstrahlung, it remains on-shell and eventually turns into hadrons. This last process obviously cannot be described by perturbative QCD. Instead, we must turn to analogies and phenomenological models.

It is natural to compare hadronization with low-p_T hadron scattering. Both processes involve energetic, nearly on-shell quanta. The comparison is also suggested by the similarity of the corresponding quark diagrams. The diagram of Fig. 18a actually suggests that e^+e^-

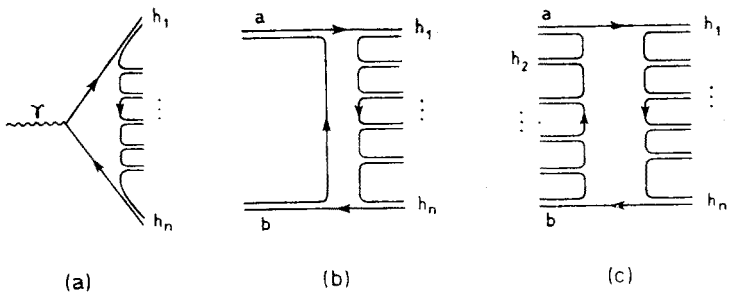

Fig. 18. Quark diagrams for (a) $e^+e^- \to$ hadrons. (b) ab $\to$ hadrons (meson exchange). (c) ab $\to$ hadrons (pomeron exchange)

annihilation should be simpler than hadron collisions, there being only one quark line that emits hadrons. In the dominant process of soft collisions (Pomeron exchange), hadrons are emitted simultaneously, from two quark lines (Fig. 18c). There have been many attempts to calculate hadron production in low-p_T scattering using e^+e^- data, often with encouraging success. A good review was recently given by Diebold [42].

Do the present e^+e^- data support the existence of a plateau in rapidity $Y = \frac{1}{2}\log\left(\frac{E+p_L}{E-p_L}\right)$, as the quark diagram would suggest? The SPEAR data indicated [1] the formation of a plateau, with a central density of ~ 1.5 charged particles per unit rapidity at $Q \simeq 7.7$ GeV. This has also been observed [43] at DORIS ($Q = 9.4$ GeV). Higher energy PETRA data, while still preliminary, are consistent with a lengthening plateau [44]. A plateau height of ~ 1.8 has also been measured in ν induced jets at Fermilab [45].

At the energies considered, the fragmentation is likely to be dominantly non-perturbative (cf. Sections 2 and 4). Hence the existence of a plateau supports the analogy to soft collisions. The height of the e^+e^- plateau is somewhat larger than naively expected, however. The plateau height in pp collisions [46] has some energy dependence, increasing from ~ 1.5 at $\sqrt{s} = 20$ GeV to ~ 2.1 at $\sqrt{s} = 63$ GeV. This is still consistent with approaching twice the e^+e^- value from below [47]. It is, however, also possible that branching processes enhance the multiplicity in e^+e^- annihilations. This effect should grow in importance as the energy increases.

It will clearly be of importance for experiments at PETRA and PEP to investigate the existence and properties of a rapidity plateau. Apart from its height, one should consider other features, such as correlation lengths and the distribution of gaps in rapidity. In hadron collisions, these are determined by the probability for a quark line to extend over a long range in rapidity without emitting hadrons, and given by Regge behaviour. Present data is consistent with similar behaviour in quark jets [48]. On the other hand, the quark diagram of Fig. 18a suggests a simpler picture for e^+e^-. Flavour correlations between hadrons arise when they share the same quark line. Since the single quark line cannot emit hadrons, the gap and correlation lengths should be the same. By contrast, in hadron collisions the gaps are shorter because *two* quark lines must not emit. We return to these questions below in the context of specific models.

II. The quark cascade model

The general questions posed above are often difficult to answer experimentally, because of limited statistics or acceptance. Thus it is useful also to consider explicit models that describe the entire event. Acceptance corrections can then be applied directly to the model predictions.

The quark cascade model [11, 25] is by far the most commonly used model for hadronization. Particularly in the parametrization of Field and Feynman (FF) it has been widely used by experimenters and usually found to agree well with data. Here I would like first to review very briefly the essentials of the cascade model. I shall then discuss some of its (theoretical) shortcomings, most of which are well-known. These could become serious in a more detailed study of jet structure. We are thus led to consider an alternative model [10] which is free of such difficulties, and related to the well established multiperipheral picture of hadron scattering.

In the cascade model, hadrons are produced by repeated bremsstrahlung from a quark,

$$\begin{array}{l} q \to q_1 + h_1 \\ \quad\quad \hookrightarrow q_2 + h_2 \\ \quad\quad\quad\quad \hookrightarrow q_3 + h_3 \\ \quad\quad\quad\quad\quad\quad \hookrightarrow \ldots \end{array} \tag{6.1}$$

In each decay, the produced quark gets a fraction η, and the hadron $1-\eta$, of the available energy. This fraction is distributed according to a primordial fragmentation function

$f(\eta)$, with

$$\int_0^1 f(\eta)d\eta = 1,$$

The total probability (or weight) of a given decay sequence (6.1) is thus

$$W = \prod_k f(\eta_k). \tag{6.2}$$

The *rank* of a hadron refers to the production sequence. Thus hadron h_k in (6.1) has rank k. In general, the ordering in rank and rapidity need not be the same. For example, h_1 can have a small energy if $\eta_1 \simeq 1$.

To make the model "realistic", a number of further embellishments are required:

Flavour: The quark types in (6.1) are picked according to an assumed probability distribution.

Transverse momentum: The model is basically one-dimensional, but p_T can be added "by hand".

Resonances: The primary hadrons in (6.1) can be resonances (ρ, K*, ...) which subsequently decay. FF chose equal numbers of pseudoscalar and vector particles.

Having chosen the above parameters, one can fix the primordial function $f(\eta)$ from data on one-particle distributions. FF found

$$f(\eta) = 0.23 + 2.31\eta^2. \tag{6.3}$$

The model predictions can be efficiently evaluated numerically, and have turned out to be in good overall agreement with data [1, 2, 43].

The cascade model is well-defined in an infinite-momentum frame, where $E = p$ for all hadrons. When it is applied to finite energy jets there are ambiguities and inconsistencies, however. Only one combination of energy and momentum, but not both simultaneously, can be conserved at each fragmentation vertex. It is also unclear how to terminate the fragmentation as the remaining energy runs out. In practice, a lower cut-off on the quark energy is usually applied. This means, however, that the final quark and its quantum numbers are lost.

The model has a rapidity plateau. This can be seen by noting that hadrons of consecutive ranks have energies

$$\frac{E_k}{E_{k+1}} = \frac{1-\eta_k}{\eta_k(1-\eta_{k+1})}. \tag{6.4}$$

Since the ratio depends only on $f(\eta)$ in (6.3), the average particle spacing in rapidity is constant. The plateau has some unusual properties, though, which are not generally associated with plateaus in hadron collisions. First, I shall argue that the particle distribution depends on the *direction* in which the original quark was moving[16]. This is true even

[16] An argument to the same effect was given in Ref. [11].

inside the plateau region, where one normally would think that the hadrons are independent of end effects, due to short range correlations.

Consider the event shown in Fig. 19. The particles are labelled according to rank and ordered on the rapidity axis. They are to be thought of as only a part of the full distribution, with many more hadrons situated to the left and to the right. I shall show that the likelihood for generating this sequence in the cascade model depends on whether the original

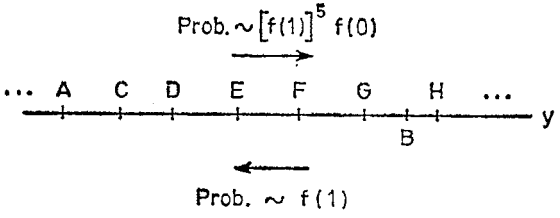

Fig. 19. A rapidity plot of hadrons A, B, ..., H produced in the cascade model. The arrows indicate the direction in which the original quark was moving

quark moved to the left (i.e., hadron A is the most energetic one shown) or to the right (in which case H is lowest in rank).

The sequence in Fig. 19 has one unusual feature: the rapidity of B is very different from what its order in rank would normally imply. If the initial quark moved to the left, this could happen if B is produced with $\eta \approx 1$, i.e. this hadron obtains only the small fraction $1-\eta$ of the available energy. The quark produced with B is then energetic, and produces C at the typical rapidity distance from A. The remaining hadrons D, E, ... are also produced with typical energies. The "improbability" of the event is thus measured by $f(1)$, the likelihood for one fragmentation with $\eta \approx 1$.

The picture is quite different if the original quark moved to the right in Fig. 19. The decay sequence looks normal until, after C, hadron B is suddenly produced with a very much higher energy. After this, hadron A (and the following ones) are at typical distances *from C*. This can happen only provided all of the hadrons G, F, E, D, C are produced with $\eta \approx 1$, so that energy is stored in the quark. Then the quark must, in one decay, give up almost all its energy to B: $\eta \approx 0$. The "improbability" is now $[f(1)]^5 f(0)$, clearly different from what we found previously.

The above argument shows that the hadron distribution depends on the direction in which it is generated. If in e^+e^- annihilation two back-to-back jets are generated, the point $y_{CM} = 0$ will be very special. This is not what one would expect in a hadronization picture with short range correlations.

There is also another unexpected feature of the plateau distribution. We saw above that although hadron B in Fig. 19 was produced far from A, the next particle (C) was nonetheless close to A. The generating procedure "remembers" more than just the position of the last hadron. This is again different from multiperipheral-Regge models, in which a rapidity gap, once created, normally is not again populated.

Most of the effects discussed here are likely to be small, and would reveal themselves

only in a detailed study of the events. It is also possible that the cascade model is correct and, e.g., the distributions *are* different on the two sides of $y_{CM} = 0$ in $e^+e^- \to$ hadrons. In either case, it is useful to consider alternative models, more in line with the phenomenology of hadron scattering. I shall next discuss a model based on the multiperipheral scheme.

III. A model for quark hadronization [10]

As in the cascade model, we consider the quark diagram of Fig. 18 in 1 + 1 dimensions. The total weight is written as a product, like in (6.2). However, each factor $h(y)$ is now associated with a quark line, and depends on the distance y that this quark line extends in rapidity. From short range correlation and Regge behaviour we expect

$$h(y) \sim \exp(-\alpha y) \quad \text{as} \quad y \to \infty. \tag{6.5}$$

The function h is otherwise unknown. It may include resonance effects for small y.

The weight of an n-particle event is thus

$$W_n = \prod_{k=1}^{n+1} h(|y^{(k)} - y^{(k-1)}|), \tag{6.6}$$

where $y^{(k)}$ is the rapidity of the hadron of rank k. $y^{(0)}$ and $y^{(n+1)}$ are the rapidity positions of the initially produced quarks. They should be outside the rapidity range populated by hadrons, but are otherwise unimportant parameters. Note that the order in rank and rapidity can be different. The absolute sign in (6.6) ensures that the weight only depends on the (absolute) distance between the hadrons that the quark line connects.

The n-particle cross-section is obtained[17] by integrating the weight (6.6) over phase space, subject to energy-momentum conservation:

$$\sigma_n = \int_{-\infty}^{\infty} dy_1 \int_{y_2}^{\infty} dy_2 \ldots \int_{y_n-1}^{\infty} dy_n \sum_{\text{Perm}} \prod_{k=1}^{n+1} h(|y^{(k)} - y^{(k-1)}|) \delta^{(2)}(\sum_1^n p_i - p). \tag{6.7}$$

Here $y_1, \ldots, y_n$ is the ordered set of hadron rapidities. The sum is over all $n!$ ways of assigning ranks to the hadrons, thus determining the rank rapidities $y^{(k)}$.

The model defined by (6.7) has several advantages compared to the cascade model. Momentum conservation is exact. There is no ambiguity or loss of slow particles. The condition (6.5) implies short range correlations and hence a forward-backward symmetric plateau. There is nothing special about $y_{CM} = 0$.

Furthermore, resonance effects can at least partly be described by the form of $h(y)$ at small y. It may thus be sufficient to consider only the production of stable particles in (6.7). In this respect the situation is analogous to that in hadron collisions: resonances are "dual" to quark exchange.

The fragmentation of heavy quarks is believed to be different from that of light quarks, with the heavy hadron taking most of the energy [49]. In a cascade picture, this feature has to be put in "by hand" via the primordial function $f(\eta)$. In a rapidity formulation such

---

[17] I am assuming only one quark flavour. Several flavours can be incorporated as in the cascade model.

sa (6.7), on the other hand, it emerges naturally. The separation *in rapidity* between light and heavy hadrons is the typical one, given by the extension of light quarks. This implies that the heavy hadron will take most of the momentum, because of the mass dependence in $y = \log\left(\frac{E+p_{\|}}{m_T}\right)$.

It must be said, though, that these good features were obtained at the expense of calculational simplicity. The weight in (6.7) is a sum of $n!$ terms. Even though most of these will be quite small, there remains the problem of sorting out and summing the important ones. Fortunately, this draw-back is alleviated by the (rather surprising) fact that the properties of the plateau region can be calculated exactly and analytically, in the case $h(y) = g\exp(-\alpha y)$. I shall next describe this solution. Quite apart from its relevance for jets, I think this feature makes the model interesting to study.

Since the particles in the plateau region carry negligible energy, we may drop the energy-momentum δ-function in (6.7). Substituting also $h(y) = g\exp(-\alpha y)$ (and dropping an overall factor of g) we have

$$\sigma_n = g^n \int_{-\infty}^{\infty} dy_1 \int_{y_1}^{\infty} dy_2 \ldots \int_{y_{n-1}}^{\infty} dy_n \sum_{\text{Perm}} \exp\left[-\alpha \sum_{k=1}^{n+1} |y^{(k)} - y^{(k-1)}|\right]. \tag{6.8}$$

The plateau region of this simplified model (which as we shall see extends from $y^{(0)}$ to $y^{(n+1)}$) should be identical to the plateau of the original model (6.7). The hadron rapidities in (6.8) can range beyond $[y^{(0)}, y^{(n+1)}]$, but in this region momentum conservation cannot be ignored.

I shall begin by reformulating the cross-section (6.8). For convenience I take $y^{(0)} = 0$ and $y^{(n+1)} = Y$. The weight of a given configuration depends only on the total rapidity distance travelled by the quark lines. As shown in Fig. 20, we may characterize the quark

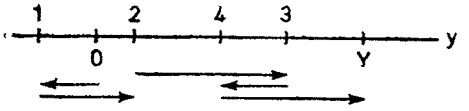

Fig. 20. Rapidity plot of a 4-particle event. The arrows show the movement of the quark lines

lines as going "forward" (left to right) or "backward". If there are no lines going backward the total distance travelled is Y and

$$\sigma_n^{(0)} = g^n \int_0^Y dy_1 \int_{y_1}^Y dy_2 \ldots \int_{y_{n-1}}^Y dy_n \exp(-\alpha y) = e^{-\alpha Y} g^n Y^n / n! \tag{6.9}$$

This is nothing but the well-known Chew–Pignotti model [50].

Now assume there are m lines moving backward a combined distance Δ. The total distance travelled by all lines is then $Y+2\Delta$. There are $\binom{n+1}{m}$ ways of choosing the m backward-moving lines from the $n+1$ quark lines. The phase space integral over all

divisions of Δ into m intervals and of $Y+\Delta$ into $n+1-m$ intervals can be done explicitly as in (6.9). The total n-particle cross-section is thus

$$\sigma_n = g^n e^{-\alpha Y}\left[\frac{Y^n}{n!} + \sum_{m=1}^{n}\binom{n+1}{m}\int_0^\infty d\Delta e^{-2\alpha\Delta}\frac{\Delta^{m-1}}{(m-1)!}\frac{(Y+\Delta)^{n-m}}{(n-m)!}\right]. \tag{6.10}$$

This expression can be further simplified by expanding $(Y+\Delta)^{n-m}$ and doing the integral over Δ. By means of the identity

$$\sum_{m=1}^{n-k}\binom{n+1}{m}\binom{n-k-1}{m-1} = \binom{2n-k}{n-k}$$

one finds

$$\sigma_n = g^n e^{-\alpha Y}\sum_{k=0}^{n}(2\alpha)^{k-n}\binom{2n-k}{n-k}Y^k/k!. \tag{6.11}$$

Consider now the total cross-section

$$\sigma_T = \sum_{n=0}^{\infty}\sigma_n.$$

If the order of the sums over n and k in (6.11) is reversed one gets a sum involving the hypergeometric functions $F(\frac{1}{2}k+\frac{1}{2}, \frac{1}{2}k+1; k+1; 2g/\alpha)$. These can be expressed using elementary functions [51]. The final sum over k gives the remarkably simple result

$$\sigma_T = \frac{1}{\lambda}\exp(-\lambda\alpha Y), \tag{6.12}$$

where

$$\lambda = \sqrt{1-2g/\alpha}. \tag{6.13}$$

It is interesting to note that σ_T blows up as $\lambda \to 0$, or $\alpha \to 2g$. A singularity of this kind could have been anticipated already from (6.8). As $\alpha \to 0$, this expression reduces to a phase space integral over an infinite volume, which is necessarily divergent. (Similarly, (6.7) becomes a standard phase space model with momentum conservation.) From (6.12) and (6.13) we learn that the "phase transition" occurs already at $\alpha = 2g$. As we shall see, long range correlations arise at this point, and the hadrons spread over the whole rapidity axis. The expression (6.8) is meaningless for $\alpha \leqslant 2g$, while the original model (6.7) is still well-defined (but has no rapidity plateau with short range correlations!).

Because of the factor g^n in (6.11), σ_T is actually a multiplicity generating function. It is likewise easy to find $\langle m\rangle$ and $\langle\Delta\rangle$, the average number of backward-moving lines and the average distance they extend:

$$\langle n\rangle = \frac{1}{\lambda}gY + \frac{1-\lambda^2}{2\lambda^2},$$

$$\langle m\rangle = \frac{1-\lambda}{2\lambda}\left[gY + \frac{2\lambda^2+\lambda+1}{2\lambda}\right],$$

$$\langle \Delta\rangle = \frac{(1-\lambda)^2}{4\lambda}\,Y + \frac{1-\lambda^2}{4\alpha\lambda^2}. \tag{6.14}$$

As $\lambda \to 0$, there are, on the average, as many backward- as forward-moving lines, and the distance they cover tends to infinity.

The inclusive particle distributions can be obtained very simply from σ_T. The probability for finding a particle (of any rank) at y is equal to the total probability for the quark lines to migrate from 0 to y, times the probability that they make it from y to Y:

$$\frac{1}{\sigma_T(Y)}\frac{d\sigma}{dy} = \frac{g}{\sigma_T(Y)}\sigma_T(y)\sigma_T(Y-y). \tag{6.15}$$

Using (6.12), this is a plateau of height g/λ from 0 to Y, which for $y < 0$ is cut off as $(g/\lambda)\exp(2\alpha\lambda y)$. The cut-off for $y > Y$ is analogous (Fig. 21). Recalling that momentum is not conserved in (6.8), this decrease just reflects the correlation length.

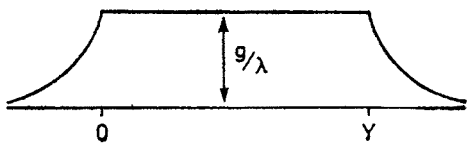

Fig. 21. Hadron rapidity distribution in the model (6.8)

The two-particle distribution can also be expressed in terms of σ_T. Subtracting a product of single-particle distributions (6.15) we have for the correlation function of two particles at y_1, y_2 $(0 < y_1 < y_2 < Y)$:

$$\varrho(y_1, y_2) = \frac{g^2}{\lambda^2}\exp\left[-2\alpha\lambda(y_2-y_1)\right]. \tag{6.16}$$

From this we can see that the correlation length is $1/(2\alpha\lambda)$, and indeed diverges as $\lambda \to 0$.

Let us finally consider the case of two particles in the central region that have consecutive ranks. The probability for a quark line to propagate from y_1 to y_2 without emitting hadrons is $\exp\left[-\alpha(y_2-y_1)\right]$. Hence the two-particle distribution is

$$\frac{1}{\sigma_T}\frac{d\sigma}{dy_1 dy_2} = \frac{g^2}{\lambda}\exp\left[-\alpha(1-\lambda)(y_2-y_1)\right]\left[1+\exp\left(-2\alpha\lambda(y_2-y_1)\right)\right]. \tag{6.17}$$

The second term corresponds to the possibility that the hadron at y_2 has lower rank. It can be neglected when $y_2 - y_1 \gg 1/(2\alpha\lambda)$.

As noted previously, the multiplicity is lower than average in the region between two hadrons of consecutive rank. The single quark line separating them is not emitting hadrons. Eq. (6.17) reminds us, however, that this is an asymptotic prediction, valid for large $y_2 - y_1$.

The second term in (6.17) in fact gives rise to twice the average multiplicity. This enhancement at small separations is linked to the positive correlation (6.16).

As the above examples show, the model defined by (6.8) has some very simple, yet non-trivial properties. It can be regarded as a natural generalization of the multiperipheral model proposed by Chew and Pignotti [50]. We allow quark lines to go "backward", so that the order in rank and rapidity can be different. As $\alpha \to \infty$ such backward steps are suppressed and our model (6.11) reduces to that of Chew and Pignotti, Eq. (6.9).

7. Concluding remarks

Jet studies can shed light on a wide range of strong interaction phenomena. At present, one of the most interesting questions is whether experimental evidence will be found for multi-jet structure. This would provide a direct test of QCD perturbation theory. As was emphasized first by Sterman and Weinberg [6], the perturbation expansion *is* reliable for properly inclusive "jet" cross-sections. In Section 4 we estimated the energy range at which hard gluon bremsstrahlung should become visible in e^+e^- annihilations, based on known properties of the non-perturbative hadronization. The p_T broadening sets in at $Q \approx 15$ GeV, and is a major effect by $Q = 30$ GeV. It would thus seem that data from PETRA and PEP will be decisive in this regard.

The structure of individual jets can be calculated in the leading logarithm approximation (l.l.a.), which is valid for small angles between the partons. The success [35] of the l.l.a. in predicting scaling violations for deep inelastic lepton scattering makes this particularly interesting. Furthermore, in jets one can go beyond the single-parton distribution to discuss correlations and global properties of the events. In the l.l.a., perturbation theory reduces to a branching process. We made use of this in Section 5 to investigate the event structure in terms of branching probabilities.

Compared to deep inelastic scattering, the situation in jet physics is complicated by the fact that hadron, rather than parton, distributions are observed experimentally. Therefore some assumption is required concerning how partons turn into hadrons, in order to compare with data on jet structure. (For inclusive quantities such as total jet production cross-sections this is not required, since one sums over an essentially complete set of states.) As I discussed in Section 6, it is natural to compare hadronization with low p_T scattering phenomena. More data on rapidity distributions, gaps and correlations would help to clarify this question.

I am very grateful to the organizers of this school for inviting me to attend. The preparation of my lectures rests on the many fruitful discussions and collaborations I have had with K. Konishi, T. F. Walsh, P. Zerwas and with my colleagues at the Niels Bohr Institute and Nordita. Special thanks go to N. Sakai for reading the manuscript.

REFERENCES

[1] G. Hanson et al., *Phys. Rev. Lett.* **35**, 1609 (1975); G. Hanson, Proceedings of the 13th Rencontre de Moriond, Les Arcs, March 1978, Vol. II, p. 15.

[2] Ch. Berger et al., *Phys. Lett.* **78B**, 176 (1978) and **82B**, 449 (1979).

[3] Proceedings of the Symposium on Jets in High Energy Collisions, Copenhagen, July 1978, *Phys. Scr.* **19**, 65 (1979).
[4] Ch. Berger et al., *Phys. Lett.* **81B**, 410 (1979); R. Brandelik et al., *Phys. Lett.* **83B**, 261 (1979).
[5] H. D. Politzer, *Phys. Rep.* **14C**, 129 (1974); W. Marciano, H. Pagels, *Phys. Rep.* **36**, 137 (1978).
[6] G. Sterman, S. Weinberg, *Phys. Rev. Lett.* **39**, 1436 (1977).
[7] R. P. Feynman, *Photon-Hadron Interactions*, W. A. Benjamin Inc., New York 1972.
[8] P. Hoyer, P. Osland, H. G. Sander, T. F. Walsh, P. M. Zerwas, DESY preprint 79/21 (1979).
[9] P. Cvitanović, P. Hoyer, K. Konishi, *Phys. Lett.* **85B**, 413 (1979).
[10] P. Hoyer, C.-H. Lai, J. L. Petersen, Nordita preprint 79/22 (1979).
[11] R. D. Field, R. P. Feynman, *Nucl. Phys.* **B136**, 1 (1978).
[12] A. Ali, J. G. Körner, G. Kramer, J. Willrodt, *Z. Phys.* **C1**, 203 (1979).
[13] G. Drews et al., *Phys. Rev. Lett.* **41**, 1433 (1978).
[14] M. G. Albrow et al., *Nucl. Phys.* **B160**, 1 (1979).
[15] B. H. Wiik, Review talk at the Neutrino 1979 meeting in Bergen, June 1979; P. Söding, Invited talk at the EPS International Conference on High Energy Physics, Geneva, June 1979.
[16] D. H. Perkins, Review talk at the Neutrino 1979 meeting in Bergen, June 1979.
[17] J. Ellis, Proceedings of the SLAC Summer Institute on Particle Physics, July 1978, SLAC-215, p. 69; H. D. Politzer, Proceedings of the 19th International Conference on High Energy Physics, Tokyo 1978, p. 229; A. De Rújula, ibid., p. 236.
[18] D. Amati, R. Petronzio, G. Veneziano, *Nucl. Phys.* **B146**, 29 (1978).
[19] A. De Rújula, J. Ellis, E. G. Floratos, M. K. Gaillard, *Nucl. Phys.* **B138**, 387 (1978).
[20] Yu. L. Dokshitzer, D. I. D'yakonov, S. I. Troyan, Proceedings of XIII Winter School of LNPI, Leningrad 1978, Vol. I; English translation, SLAC-TRANS-183 (1978); C. H. Llewellyn Smith, Lectures presented at the XVII Internationale Universitätswochen für Kernphysik, Schladming, Austria 1978, published in *Acta Phys. Austriaca, Suppl.* XIX, 331 (1978); G. Altarelli, Invited talk at the Topical Conference on Neutrino Physics at Accelerators, Oxford, July 1978, INFN-Rome preprint no. 714; C. T. Sachrajda, Proceedings of 13th Rencontre de Moriond, Les Arcs, March 1978, Vol. I, p. 17; D. Amati, Lecture given at the 4-th Rencontre de Moriond, Les Arcs, March 1979 CERN TH. 2650.
[21] T. E. Harris, The Theory of Branching Processes, Springer, Berlin 1963; K. B. Athreya, P. E. Ney, Branching Processes, Springer, Berlin 1972.
[22] R. K. Ellis, R. Petronzio, *Phys. Lett.* **80B**, 249 (1979); K. Konishi, A. Ukawa, G. Veneziano, *Phys. Lett.* **80B**, 259 (1979).
[23] J. Wosiek, K. Zalewski, Cracow preprint (1979); W. Furmański, CERN preprint TH. 2664 (1979).
[24] A. M. Polyakov, *Sov. Phys. JETP* **32**, 296 (1971); **33**, 850 (1971).
[25] A. Seiden, *Phys. Lett.* **68B**, 157 (1977); B. Andersson, G. Gustafson, C. Peterson, *Nucl. Phys.* **B135**, 273 (1978); U. Sukhatme, *Phys. Lett.* **73B**, 478 (1978).
[26] A. Krzywicki, B. Petersson, *Phys. Rev.* **D6**, 924 (1972).
[27] T. Kinoshita, *J. Math. Phys.* **3**, 650 (1962); T. D. Lee, M. Nauenberg, *Phys. Rev.* **133**, B1549 (1964).
[28] P. M. Stevenson, *Phys. Lett.* **78B**, 451 (1978); B. G. Weeks, *Phys. Lett.* **81B**, 377 (1979); P. Binétruy, G. Girardi, *Phys. Lett.* **83B**, 382 (1979).
[29] C. L. Basham, L. S. Brown, S. D. Ellis, S. T. Love, *Phys. Rev.* **D17**, 2298 (1978).
[30] I. I. Y. Bigi, T. F. Walsh, *Phys. Lett.* **82B**, 267 (1979).
[31] J. Ellis, M. K. Gaillard, G. Ross, *Nucl. Phys.* **B111**, 253 (1976); T. DeGrand, Y. J. Ng, S.-H. Tye, *Phys. Rev.* **D16**, 3251 (1977).
[32] S.-Y. Pi, R. L. Jaffe, F. E. Low, *Phys. Rev. Lett.* **41**, 142 (1978); G. Kramer, G. Schierholz, J. Willrodt, *Phys. Lett.* **79B**, 249 (1978) and erratum, **80B**, 433 (1979); J. Ellis, I. Karliner, *Nucl. Phys.* **B148**, 141 (1979).
[33] E. Farhi, *Phys. Rev. Lett.* **39**, 1587 (1977).

[34] G. Kramer, G. Schierholz, *Phys. Lett.* **82B**, 108 (1979).
[35] P. Bosetti et al., *Nucl. Phys.* **B142**, 1 (1978); H. L. Anderson et al., *Phys. Rev. Lett.* **40**, 1061 (1978); J. G. H. de Groot et al., *Phys. Lett.* **82B**, 292 and 456 (1979); D. W. Duke, R. G. Roberts, Rutherford preprint RL-79-025 (1979).
[36] I. V. Andreev, P. N. Lebedev Physical Institute, preprint 1979; A. Giovannini, Univ. of Torino, preprint 1979.
[37] L. N. Lipatov, *Yad. Fiz.* **20**, 181 (1974) (*Sov. J. Nucl. Phys.* **20**, 94 (1975)).
[38] G. Altarelli, G. Parisi, *Nucl. Phys.* **B126**, 298 (1977).
[39] K. Konishi, A. Ukawa, G. Veneziano, *Phys. Lett.* **78B**, 243 (1978) and *Nucl. Phys.* **B157**, 45 (1979).
[40] J. Wosiek, K. Zalewski, *Acta Phys. Pol.* **B10**, 667 (1979).
[41] J. C. Taylor, *Phys. Lett.* **73B**, 85 (1978).
[42] R. Diebold, Proceedings of the 19th International Conference on High Energy Physics, Tokyo 1978, p. 666.
[43] G. Flügge, Lectures presented at the XVIII Internationale Universitätswochen für Kernphysik, Schladming, Austria 1979, DESY preprint 79/26.
[44] K. Wacker, Invited talk at the Nordic Particle Physics Meeting, Copenhagen, April 1979.
[45] J. C. Vander Velde, p. 173 of Ref. [3].
[46] H. Bøggild, T. Ferbel, *Ann. Rev. Nucl. Sci.* **24**, 451 (1974); K. Guettler et al., *Phys. Lett.* **64B**, 111 (1976); W. Thomé et al., *Nucl. Phys.* **B129**, 365 (1977).
[47] A. Capella, U. Sukhatme, Chung-I Tan, J. Tran Thanh Van, *Phys. Lett.* **81B**, 68 (1979).
[48] P. Hoyer, C. Peterson, C.-H. Lai, J. L. Petersen, *Nucl. Phys.* **B151**, 389 (1979).
[49] M. Suzuki, *Phys. Lett.* **71B**, 139 (1977); J. D. Bjorken, *Phys. Rev.* **D17**, 171 (1978).
[50] G. F. Chew, A. Pignotti, *Phys. Rev.* **176**, 2112 (1968).
[51] M. Abramowitz, I. A. Stegun, *Handbook of Mathematical Functions*, Dover, New York 1965 p. 556.